Journal of Sustainability Science and Management
Volume 20 Number 1, January 2025: 164-178
eISSN: 2672-7226

THE EFFECT OF NORTHEAST MONSOON ON THE PHYSICAL-CHEMICAL PARAMETERS AND DFE(III) IONS AT PULAU REDANG, TERENGGANU

NUR JANNATI RAMJAM, KHAIRUL NIZAM MOHAMED* AND MUHAIMIN AMIRUDDIN

Department of Environment, Faculty of Forestry and Environment, Universiti Putra Malaysia, 43400 Serdang, Selangor, Malaysia.

**Corresponding author: k_nizam@upm.edu.my*
http://doi.org/10.46754/jssm.2025.01.010
Received: 1 August 2023 *Accepted: 15 September 2024* *Published: 15 January 2025*

Abstract: The physical-chemical parameters and dissolved Fe(III) ion distribution [dFe(III)] were determined throughout the water column at Pulau Redang, Terengganu. This study was carried out in March 2019 and October 2019 to evaluate the possible effect of the northeast monsoon (NEM) on the pH, salinity, dissolved oxygen, turbidity, conductivity, and dFe(III) ion concentration. The determination of dFe(III) ion was carried out by using the optimised adsorptive-cathodic stripping voltammetry (AdCSV) method. The results show a change in physical and chemical conditions between March 2019 and October 2019 is due to the seasonal northeast monsoon phenomenon. However, the dFe(III) ion concentrations did not differ significantly ($p > 0.05$) in March 2019 and October 2019. This indicates that the NEM does change the physical-chemical condition of the water column and has no effect on the distribution of Fe(III) ions in our study area.

Keywords: Bioavailability, coastal water, dissolved Fe(III) ion, physical-chemical parameters, voltammetry.

Introduction

Northeast monsoon (NEM) is colloquially called the "winter season in Malaysia". It brings north-easterly winds up to ≥ 30 knots from early November until the end of March (Mohamed & Amil, 2015). During NEM, the eastern part of Peninsular Malaysia (e.g., Kelantan, Terengganu, Pahang, East of Johor, and some parts of Sarawak) receive heavy rainfall (Suhaila *et al*., 2010) and severe floods often occur.

Previous studies (Adiana *et al*., 2014; Godon & Mohamed, 2016) state that NEM encouraged the re-suspension of coastal sediments due to increased rapid mixing or coastal upwelling inside the water column. Sea surface temperature (SST) satellite data has also demonstrated the existence of coastal upwelling during NEM (Zainol & Akhir, 2016). D'Croz & O'Dea (2007) claim that the presence of cooler, saltier water initiated the upwelling, driving the nutrient-rich water onto the upper layer of seawater. It was proposed that this phenomenon would raise the trace metal concentration (both in particulate and total dissolved phase) (Adiana *et al*., 2014; Godon & Mohamed, 2016) and enhance the phytoplankton growth in coastal environments (Mohamed & Amil, 2015).

Another concern about NEM is its potential to alter the physical-chemical characteristics of seawater, especially dissolved oxygen (DO), salinity, and pH (Godon & Mohamed, 2016). This change was found to affect the trace metals' speciation and influence their biogeochemical cycle (Godon *et al*., 2018). During this study, we are focusing on the dissolved Fe due to its main function in promoting the growth of primary phytoplankton and becoming a significant factor in ocean productivity and the global carbon cycle (Martin *et al*., 1991; Klunder *et al*., 2011).

The existence of dissolved iron (dFe) in two metal types is widely recognised, which are Fe(II) and Fe(III) (Liu & Millero, 2002). In a coastal environment, Fe(II) is rapidly oxidised to Fe(III) due to the natural seawater pH and oxygenated conditions (Millero, 1998; Lis *et al*., 2015). Fe(III) is thermodynamically stable; however, insoluble in water due to the formation of Fe oxy-hydroxide precipitate (Achterberg *et al*., 2001). The solubility of Fe(III) can be

increased by the chelation of organic ligands produced by marine microbes (Hunter & Boyd, 2007) and/or by the sediment pore-water (Jones *et al*., 2011). Thus, it was proposed that the solubility of Fe(III) controlled the amount of Fe available in coastal waters (Johnson *et al*., 1997; Liu & Millero, 2002).

Ramjam and Mohamed (2022) found an extremely low concentration of dFe(III) ion at Pulau Redang, Terengganu in both dissolved (0.45 µm) and small colloidal (0.20 µm) Fe form. This low concentration of dFe(III) ion was expected due to increased Fe scavenging during a sediment re-suspension (Jones-Lee & Lee, 2005). This process was suggested to enhance the formation of particulate Fe (Pan *et al*., 2011). This study aims to assess the impact of the northeast monsoon on the distribution of dFe(III) and physical-chemical characteristics because the study area was impacted by NEM every year. The analysis was done in March 2019 and October 2019. To accomplish our goal, we analysed the physical-chemical parameters (pH, salinity, temperature, dissolved oxygen, conductivity, and total dissolved solid) as well as the dFe(III) ions throughout both times.

Materials and Methods

Sampling was conducted at Pulau Redang, Terengganu, which is a gazetted marine park. This study area was chosen due to it being affected by NEM annually (Roseli *et al*., 2015). The vertical seawater samples (upper, middle, and bottom layer) were collected by using a Niskin water sampler in March 2019 and October 2019 at five selected stations at the different transects of Pulau Redang, as shown in Figure 1. St. 1 was at the mixing zone between freshwater and seawater, St. 2 and St. 3 faced the other marine parks (Pulau Bidong and Pulau Tioman), and St. 4 and St. 5 faced the South China Sea (SCS). The coordinate of each station was measured using GPS MAP 78s Garmin.

The samples were collected at 3 or 4 different depths based on their total depth (D), which was previously measured by using a Hondex PS-7 portable depth sounder. The samples were then poured into 1 L polytetrafluoroethylene (PTFE) bottles and were kept for further analysis. A YSI Professional Plus Multiparameter in conjunction with multi-sensor probes for salinity, pH, temperature, barometric pressure, DO, electrical conductivity (EC), and total dissolved solids (TDS) were used to measure in-situ parameters.

Sample filtration was done through a 0.20 µm pore cellulose nitrate filter membrane (Whatmann). The filtrates were stored in 250 mL of low-density polyethylene (LDPE) bottles (Nalgene) and were immediately frozen (without acidification) for dFe(III) ion analysis. Every bottle sample used in this study was cleaned in accordance with a standard procedure (Achterberg *et al*., 2001).

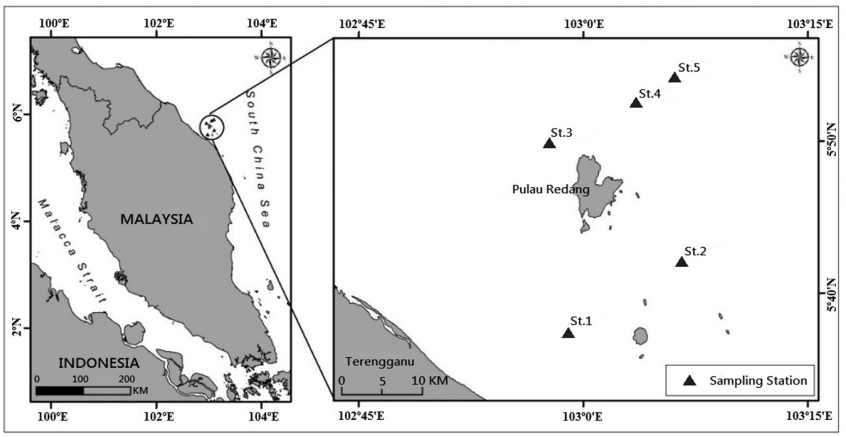

Figure 1: Sampling stations at Pulau Redang, Terengganu during March 2019 and October 2019

Adsorptive-cathodic stripping voltammetry (AdCSV) was used to determine the dFe(III) ion using voltammetry (Metrohm Model 797 VA). In this analysis, a platinum (Pt) wire was used as the counter electrode, Ag/AgCl as the reference electrode, and a hanging mercury drop electrode (HMDE) as the working electrode. The chemicals and reagents were prepared according to the protocol set by Ramjam and Mohamed (2022). A buffer solution of 0.1 M was prepared by mixing 4-(2-hydroxyethyl)-1-piperazineethanesulfonic acid (HEPES), potassium bromates (Sigma Aldrich), and NH_4OH (MERCK). This mixture buffer was equilibrated overnight with manganese oxide (MERCK) in order to remove a possible contamination of Fe ion. Methanol was used to prepare a stock solution of 0.1 M 2,3-dihydroxynaphthalene (DHN, Sigma Aldrich) which was diluted to prepare a number of Fe standards (1000 ppm, Sigma Aldrich).

The frozen sample was defrosted at room temperature and the organic content was destroyed by 2 hours of UV irradiation over the acidified sample (pH 2.0). A 10 mL of aliquot was pipetted into the quart voltammetry cell and the pH was brought back to the natural pH (8.00 to 8.10), along with the addition of 500 µL of 0.1 M HEPES/bromate (final concentration of 5 mM) buffer solution and 40 µL of 0.1 M DHN (final concentration of 400 µM). Dry nitrogen gas (purity = 99.9%) was used to purge the sample of any dissolved oxygen in 300 seconds. Deposition step was taken, where the Fe-DHN was adsorbed onto the surface of HMDE within 60 seconds (applied potential = -0.1 V). An equilibration step was allowed to occur at a differential pulse of -0.9 V to -0.1 V. Finally, the stripping current of Fe-DHN was generated at -0.60 V (± 0.05 V). The concentration of Fe(III) in the sample was determined by standard addition method.

Results and Discussion

In-situ Parameters

Table 1 shows the in-situ parameters in March 2019 and October 2019 at Pulau Redang, Terengganu, respectively. The in-situ parameters consist of salinity, temperature, pH, dissolved oxygen (DO), conductivity, and total dissolved solids (TDS). Due to the difference in the sample depth between both seasons, the in-situ parameters were divided into two categories which are the upper layer (< 15 m depth) and the lower layer (≥ 15 m depth) to ease the discussion between both seasons. The 15 m depth was chosen as the transition point between the upper and lower layers as the temperature changes were recorded at that layer.

A comparison of the in-situ parameters in March 2019 and October 2019 in our study area is shown in Figures 2 and 3, respectively. Salinity ranged from 31.6 to 32.0 psu in March 2019 and from 33.0 to 34.1 psu in October 2019, respectively (Table 1). High salinity was recorded in October 2019 [Figure 3 (a)], probably due to the low amount of precipitation and the high rate of evaporation during that season (Prabu *et al*., 2008; Saravanakumar *et al*., 2008). This is because the water temperature is warmer in October 2019 [Figure 3 (a)] compared with March 2019 [Figure 2 (a)] with a range from 28.5 to 29.8°C and between 27.9 and 28.9°C, respectively (Table 1). High temperatures increased the rate of evaporation and caused an increase in salt concentration, finally increasing the total salinity (Manikannan *et al*., 2011). In addition, there is a positive correlation between salinity and temperature (Prabu *et al*., 2008).

Meanwhile, pH varied from 7.5 to 8.0 in March 2019 (Table 3) and 7.0 to 8.1 in October 2019 (Table 4), respectively. Generally, pH remained at natural seawater pH in all sampling points. However, a low pH was recorded at St. 1 during both seasons [Figure 2(b) and Figure 3(b)]. The fluctuation of pH at St. 1 during both seasons was suggested to be due to the influence of freshwater influx (Prabu *et al*., 2008). To date, the breakdown of organic matter (OM), the decrease in temperature and salinity, and the removal of carbon dioxide (CO_2) via photosynthesis through bicarbonate degradation could potentially be the cause of the pH shift (Prabu *et al*., 2008; Saravanakumar *et al*., 2008 Mohamed *et al*., 2019).

Table 1: In-situ parameters at Pulau Redang, Terengganu, during March 2019 and October 2019 based on the upper layer (< 15 m depth) and lower layer (≥ 15 m depth)

Station	Depth (m)	Salinity (psu)		Temperature (°C)		pH		DO (mg/L)		Cond. (mS/cm)		TDS (mg/L)	
		March 2019	Oct. 2019	March 2019	Oct. 2019	March 2019	Oct. 2019	March 2019	Oct. 2019	Mach 2019	Oct. 2019	March 2019	Oct. 2019
1 (5.623'N, 102.982'E)	< 15	31.9 ± 0.1	34.0 ± 0.7	28.6 ± 0.4	28.7 ± 0.0	7.5 ± 0.1	7.0 ± 0.2	7.6 ± 0.1	5.2 ± 0.5	44.1 ± 1.4	55.1 ± 0.4	31915 ± 184	33118 ± 175
	≥ 15	32.0 ± 0.0	33.2 ± 0.0	28.9 ± 0.0	28.4 ± 0.0	7.8 ± 0.0	7.1 ± 0.0	7.1 ± 0.0	4.7 ± 0.0	52.9 ± 0.0	54.8 ± 0.0	32045 ± 121	33020 ± 104
2 (5.702'N, 103.108'E)	< 15	31.6 ± 0.0	33.9 ± 0.3	28.1 ± 0.4	29.5 ± 0.1	8.0 ± 0.0	7.4 ± 0.2	7.3 ± 0.2	5.6 ± 0.0	45.8 ± 1.0	56.4 ± 0.5	27901 ± 527	33686 ± 152
	≥ 15	31.8 ± 0.1	34.1 ± 0.0	27.9 ± 0.2	28.8 ± 0.3	8.0 ± 0.0	7.8 ± 0.0	6.8 ± 0.4	5.3 ± 0.2	41.7 ± 1.3	55.8 ± 0.2	31764 ± 153	33833 ± 147
3 (5.833'N, 102.961'E)	< 15	31.8 ± 0.2	33.0 ± 0.0	28.8 ± 0.0	29.7 ± 0.0	8.0 ± 0.0	8.1 ± 0.0	7.2 ± 0.2	5.1 ± 0.0	52.4 ± 0.3	55.1 ± 0.0	31774 ± 199	32890 ± 112
	≥ 15	31.8 ± 0.0	33.8 ± 0.2	28.8 ± 0.0	28.6 ± 0.1	8.0 ± 0.0	8.1 ± 0.0	6.9 ± 0.1	5.0 ± 0.3	52.5 ± 0.1	55.6 ± 0.0	31807 ± 161	33605 ± 138
4 (5.844'N, 103.025'E)	< 15	31.7 ± 0.0	34.0 ± 0.0	28.7 ± 0.0	29.7 ± 0.0	8.0 ± 0.0	8.0 ± 0.0	7.0 ± 0.1	5.5 ± 0.0	52.2 ± 0.0	56.7 ± 0.0	31753 ± 141	33800 ± 100
	≥ 15	31.8 ± 0.0	34.1 ± 0.0	28.4 ± 0.3	28.8 ± 0.6	8.0 ± 0.0	8.0 ± 0.0	6.7 ± 0.5	5.0 ± 0.0	52.3 ± 0.1	55.8 ± 0.6	31915 ± 192	33833 ± 175
5 (5.876'N, 103.059'E)	< 15	31.7 ± 0.0	33.8 ± 0.2	28.4 ± 0.2	29.4 ± 0.4	8.0 ± 0.0	8.0 ± 0.0	7.1 ± 0.2	5.5 ± 0.0	51.6 ± 0.6	56.4 ± 0.4	32089 ± 182	33638 ± 184
	≥ 15	31.8 ± 0.1	34.1 ± 0.0	28.3 ± 0.2	28.7 ± 0.4	8.0 ± 0.0	8.0 ± 0.0	6.8 ± 0.5	5.2 ± 0.4	51.9 ± 0.0	55.9 ± 0.6	31753 ± 138	33833 ± 146

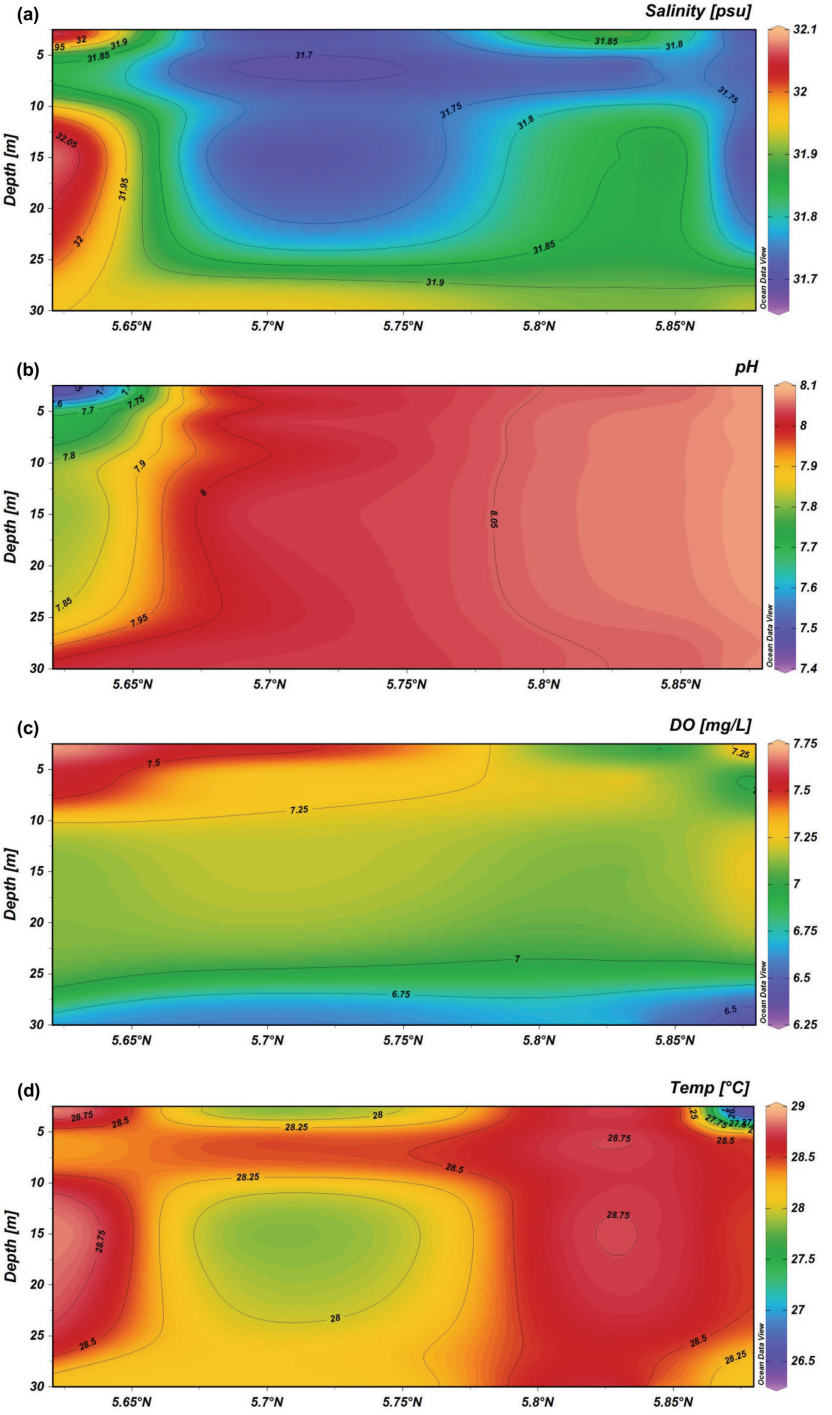
(a)
Salinity [psu]
Depth [m]
5.65°N
5.7°N
5.75°N
5.8°N
5.85°N
32.1
32
31.9
31.8
31.7
Ocean Data View
(b)
pH
8.1
8
7.9
7.8
7.7
7.6
7.5
7.4
(c)
DO [mg/L]
7.75
7.5
7.25
7
6.75
6.5
6.25
(d)
Temp [°C]
29
28.5
28
27.5
27
26.5

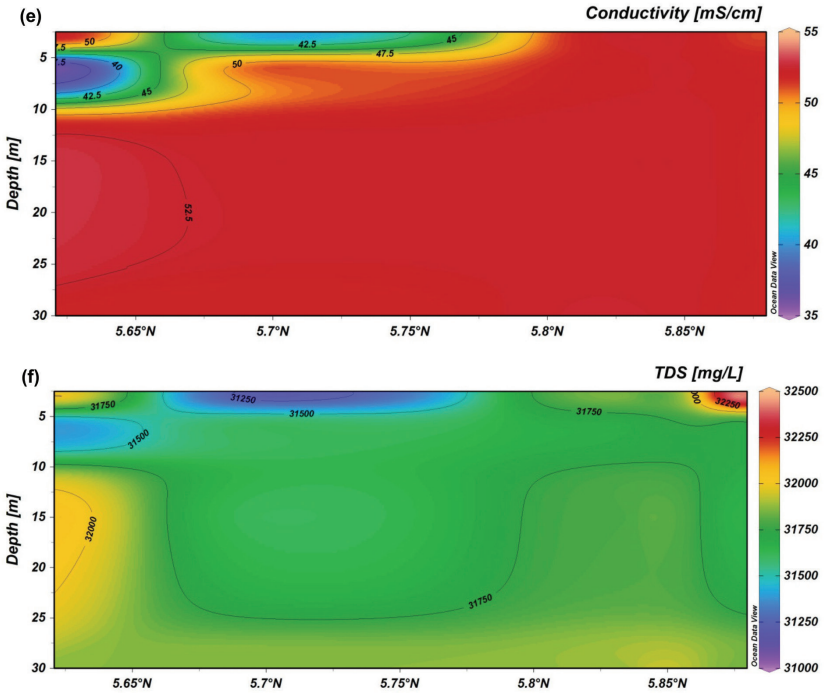

Figure 2: Cross section of in-situ parameters of all sampling locations at Pulau Redang, Terengganu during March 2019 which were (a) salinity, (b) pH, (d) dissolved oxygen, (d) temperature, (e) conductivity and (f) total dissolved solids. The dashed lines indicated the sampling stations based on their latitudes. The colour presented the reading of each parameter throughout the vertical profile

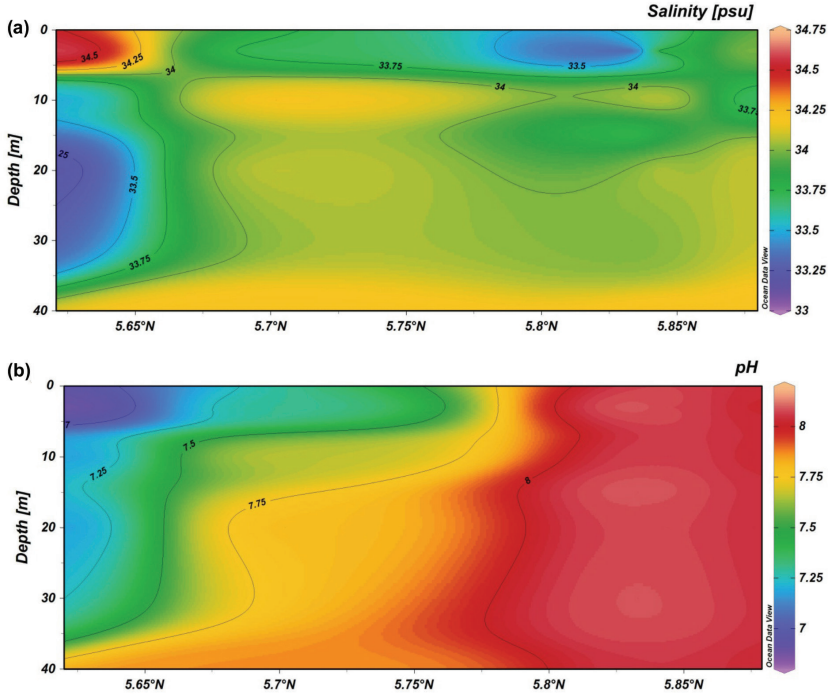

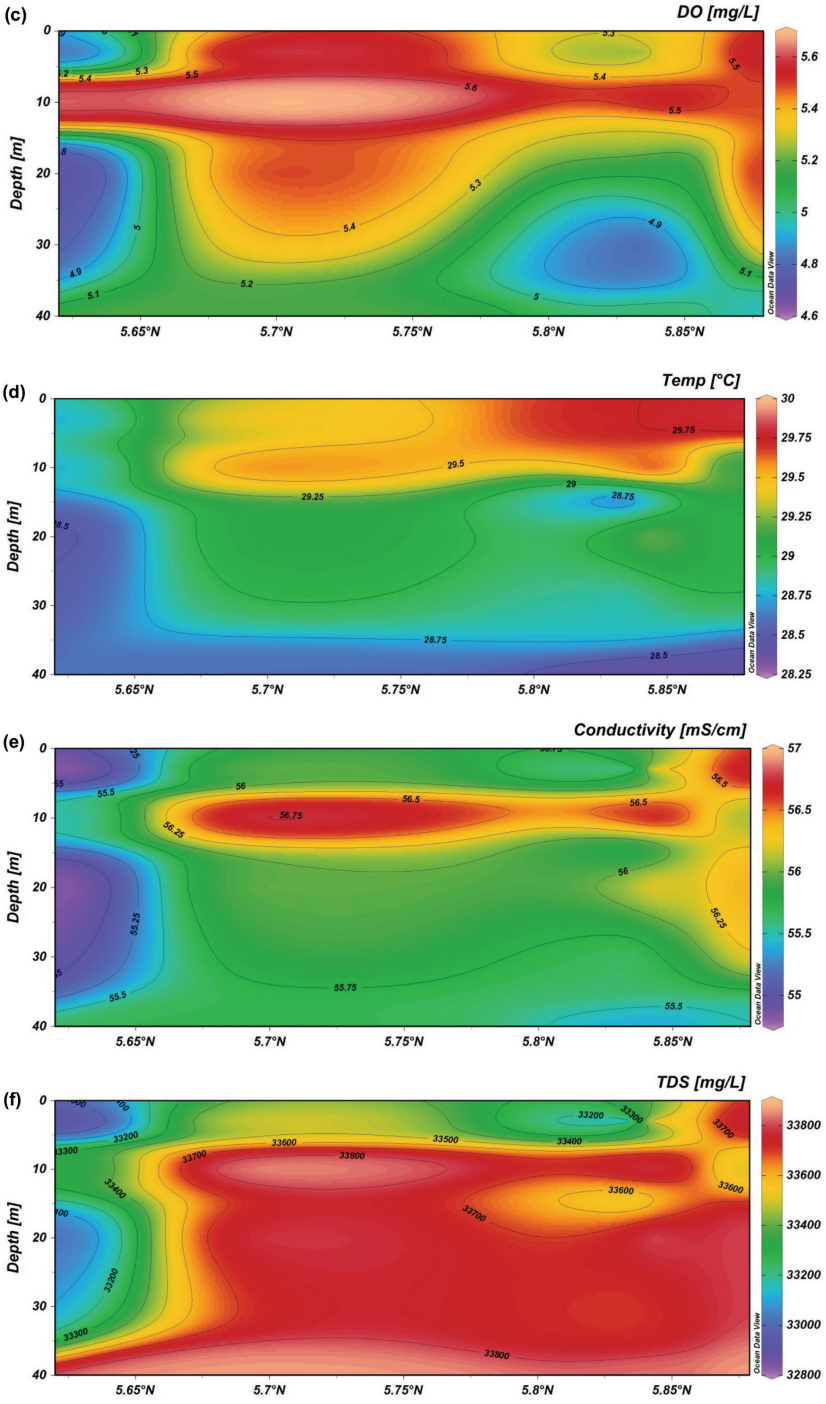

Figure 3: Cross section of in-situ parameters of all sampling locations at Pulau Redang, Terengganu during October 2019 which were (a) salinity, (b) pH, (c) dissolved oxygen, (d) temperature (e) conductivity and (f) total dissolved solids. The dashed lines indicated the sampling stations based on their latitudes. The colour presented the reading of each parameter throughout the vertical profile

Besides that, a low value of dissolved oxygen (DO) was recorded in October 2019 [Figure 3 (c)] compared with March 2019 [Figure 2 (c)] with a range of 4.7 to 5.6 mg/L and 6.7 to 7.6 mg/L, respectively (Table 1). DO plays an important role in supporting the respiration of aquatic organisms (Jack *et al*., 2009) and the dissolution is influenced by temperature and salinity (Vijayakumar *et al*., 2000). DO was found to be inversely proportional to temperature and salinity (Saravanakumar *et al*., 2008) and the hypothesis was in line with our findings. The high temperature in October 2019 [Figure 3 (d)] caused an increase in molecular vibration and reduced the amount of space available between water molecules, consequently reducing the DO (Wilson, 2010). Furthermore, the excessive salinity decreased water's ability to retain DO because its ionic charges increased competition for intermolecular space (Wilson, 2010).

The data show higher conductivity in October 2019 [Figure 3 (e)] compared with the March 2019 [Figure 2 (e)] range of 54.8 to 56.7 mS/cm and 41.7 to 52.9 mS/cm, respectively (Table 1). The high conductivity during October 2019 might have resulted from the high temperature [Figure 3 (d)], as the higher the temperature, the higher the conductivity (Barron & Ashton, 2013). This is because an increase in water temperature tends to decrease its viscosity; hence, increasing the mobility of ions in the solution (Mandal, 2014). In addition, a number of ions that enter the water column from point and/or non-point sources such as alkalis, sulfides, chlorides, and carbonates also contribute to the change in electrical conductivity (Kumar *et al*., 2015).

Total Dissolved Solids (TDS) were recorded at 32,890 to 33,832 mg/L (Table 1) in October 2019 [Figure 3 (f)], which was higher than in March 2019 [Figure 2 (f)] with 27,910 to 3,208 mg/L (Table 1). This could have been due to the high temperature (28.5 to 29.8°C) recorded in the October 2019 [Figure 3 (d)] sampling. Ngabirano *et al*. (2016) suggested that evaporation during the dry season could increase the concentration of ions, leading to the amount of TDS. Furthermore, TDS has a linear correlation with conductivity, where the increase in the concentration of dissolved ions and their ionic strength will enhance the liquid capacity to conduct an electrical charge (Shoukat *et al*., 2020).

Identification of Water Mass

A temperature-salinity (T-S) relationships of the waters of the ocean plotted on the T-S diagram serve as the immediate subject of thermohaline analysis. The analysis of the T-S relationships, together with the field expressing the equation of the state of seawater, allows taking into account the most important factors that determine the nature of the transformation and interaction of different water masses. This (T-S) diagram was used to determine how temperature, salinity, and density change with depth and to identify the vertical structure of the water column, including the water masses it contains. Plotting temperature vs. salinity data on a T-S diagram would result in a distinct and independent point for each water mass. Since each major water mass has its own characteristic range of temperatures and salinities, a water sample that falls into that range can presumably have come from that water mass (Dippner & Loick-Wilde, 2011).

There was a change in the physicochemical parameters of seawater in our study area in October 2019 and March 2019 (Figure 4), probably due to the effect of the Northeast Monsoon (NEM). Generally, the source of water mass in October 2019 was suggested to be influenced by the freshwater input, while the water mass in March 2019 was influenced by the seawater (Figure 4). This is because the pH of the water was slightly acidic (6.8 to 7.8) at the first two stations (St. 1 and St. 2) in October 2019 (Table 1). However, the pH of those stations was higher to alkaline (7.4 to 7.8) level in March 2019 (Table 1). The higher pH value in March 2019 was probably due to the seawater influx from the South China Sea (SCS).

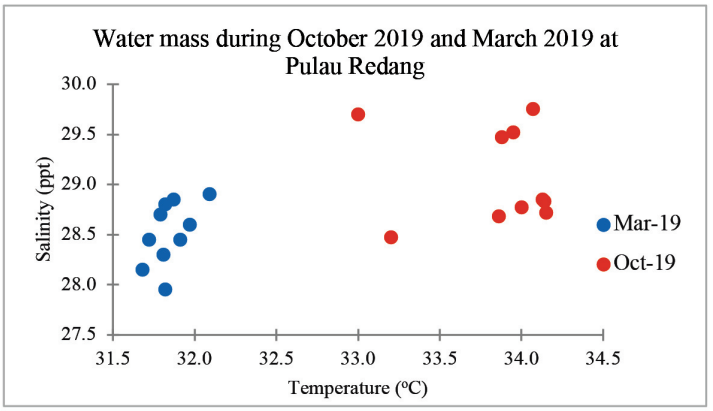

Figure 4: Temperature-Salinity (T-S) diagram for Pulau Redang in March 2019 and October 2019 at Pulau Redang, Terengganu

The temperature-salinity (T-S) diagram appeared to have different water mass characteristics between both seasons. The water mass in March 2019 lies between the T of 27.95 to 28.90°C ($\bar{x}$ = 28.52°C, n = 10) and S of 31.68 to 32.09 ppt ($\bar{x}$ = 31.85 ppt, n = 10), which were lower from October 2019 [T: 28.4 to 29.75°C ($\bar{x}$ = 29.08°C, n = 10); S: 33.20 to 34.15 ppt ($\bar{x}$ = 33.84 ppt, n = 10)]. Several studies (Anawat *et al*., 2001; Dippner & Loick-Wilde, 2011; Roseli *et al*., 2015) have categorised the water into several water masses based on their T-S characteristics. However, the water masses identified by Dippner and Loick-Wilde (2011) in Vietnamese waters (Table 2) were matched to the characteristics in our study area.

By comparing the T-S value (Table 2) to our study area, the water mass in March 2019 was probably categorised as Mekong Gulf of Thailand Water (MKGTW) which lies in T = 27 to 31°C and S = < 32.9 ppt. Meanwhile, the water mass in October 2019 is categorised as mixed water between OSW and MKGTW (WM3) due to the starting of monsoon season with T = 26 to 31°C and S = 33.7 to 34.1 ppt.

The Concentration of DFe(III)

The changing of water characteristics between March 2019 (Figure 2) and October 2019 (Figure 3) probably caused changes in the distribution of dFe(III) ions in our study area. According

Table 2: Water Mass characteristics as defined by (Dippner and Loick-Wilde, 2011) in Vietnamese water. DW = Deep water, PTW = permanent thermocline water, MSW = maximum salinity water, OSW = open sea water, MKGTW = Mekong water, WM1 = water mass 1: mixed water between MSW and PTW, WM2: mixed water between MSW and OSW, WM3: mixed water between OSW and MKGTW, and WM4: mixed water between OSW, MKGTW, and MSW

Water Mass	Temperature (°C)	Salinity (psu)
DW	< 2.5	> 34.6
PTW	7-9	34.4-34.5
MSW	17-19	> 34.3
OSW	26-31	33.7-34.1
MKGTW	27-31	< 32.9
WM1	9-17	34-35
WM2	19-28	34.1-34.6
WM3	26-31	32.9-33.7
WM4	22-26	33.3-34.1

to a study by Lin *et al*. (2018), the water's pH, salinity, and temperature all affected how soluble iron was. Hence, the data on dFe(III) ions during both seasons are presented in Table 3 and Figure 5.

Based on the Table 3, the concentration determined was 4.51 to 26.03 pM in March 2019 and 8.79 to 39.05 pM in October 2019, respectively. Statistical Package for Social Science (SPSS) software (IBM SPSS Statistics 22) was used to run an independent sample t-test at 95% confidence level of difference. The *p*-value was recorded as 0.876, which is greater than 0.05. Hence, there is no significant

Table 3: Concentration of dFe(III) during March 2019 and October 2019 at Pulau Redang, Terengganu

Station	Depth (m)	Dissolved Fe(III) (pM)	
		March 2019	October 2019
1	3	21.12 ± 0.00	8.79 ± 1.47
	6	26.03 ± 2.60	-
	10	-	19.14 ± 3.29
	15	15.63 ± 1.24	-
	20	-	15.43 ± 1.26
2	3	4.51 ± 2.00	18.79 ± 1.43
	6	10.82 ± 4.30	-
	10	-	26.16 ± 1.29
	15	20.00 ± 4.00	-
	20	-	30.91 ± 2.42
	30	5.54 ± 0.52	-
	40	-	11.18 ± 0.52
3	3	7.97 ± 2.81	19.14 ± 1.69
	6	8.20 ± 5.11	-
	15	23.89 ± 5.45	22.58 ± 5.96
	30	17.35 ± 2.47	21.20 ± 4.85
4	3	8.11 ± 5.33	16.87 ± 2.23
	6	9.67 ± 2.27	-
	10	-	24.36 ± 2.06
	15	13.35 ± 3.00	-
	20	-	39.05 ± 1.30
	30	8.37 ± 5.36	-
	40	-	15.37 ± 0.53
5	3	13.27 ± 2.12	14.33 ± 1.02
	6	7.86 ± 2.03	-
	10	-	28.52 ± 1.09
	15	16.21 ± 3.04	-
	20	-	22.08 ± 1.91
	30	8.46 ± 2.46	-
	40	-	18.44 ± 4.16

difference between the concentration of dFe(III) between March 2019 and October 2019 in our study area. The data revealed was in opposition to our current hypothesis according to a few previous data. We hypothesised that the NEM influences the distribution of nutrients (specifically dFe(III)) in the coastal water. This was supported by a strong wind (about 30 knots) that was established during NEM that was found to flush the surface sediment and bring up nutrient-rich water into the surface layer and enhance productivity (Mohamed & Amil, 2015; Godon & Mohamed, 2016).

Besides that, NEM was reported to increase the level of particulate trace metals (e.g., cadmium, chromium, lead, and manganese) in southern Terengganu during monsoon seasons (November 2007), resulting from the sediment re-suspension (Adiana *et al*., 2014). The suggestion was strengthened by Muhammad and Mohamed (2019) that 95% of Zn existed as a particulate phase during post-monsoon seasons (March 2019).

However, this present study shows that the NEM does not affect the concentration of dFe(III) ions between both seasons in our study area (Figure 5). This indicated that NEM changes only physical-chemical parameters but not the concentration of dissolved dFe(III) ions throughout the water column. Furthermore, a Fe(III) speciation study by Mohamed *et al*. (2021) reported a slightly similar distribution of [natural organic Fe(III) binding ligands/ dissolved Fe(III)] ratio (FeL/dFe) and their stability constant (Log K_{FeL}) value between October 2015 and April 2016 at the coastal water. They determined that the concentration of dissolved organic ligand (L') always exceeded the concentration of dFe(III) ions during both periods, leading to the presence of high stability of the natural organic ligand class (L_1; Log K ≈ 13). The present excess L' has saturated most of dFe(III) ions by forming a natural organic Fe(III)-ligands (FeL) complex and stabilised the distribution of Fe(III) ions in the dissolved phase. Moreover, it enhances the dFe(III) ions solubility and maintains the ions in the euphotic zone for a longer period of time (Boye *et al*., 2003; Fan, 2008). Without this strong FeL complex, the concentration of dFe(III) ions might decrease in the coastal environment (Kuma *et al*., 1996; Mohamed *et al*., 2021). This could explain the consistent concentration of dissolved Fe(III) ions in our study area during both periods.

According to Ramjam and Mohamed (2022), approximately 2 hours were needed to irradiate the samples collected in the area by using UV light to digest all the organic substances that bind to the Fe(III) ions in their analysis. Compared to other studies by Zhu *et al*. (2018), Abualhaija *et al*. (2015), and Boye *et*

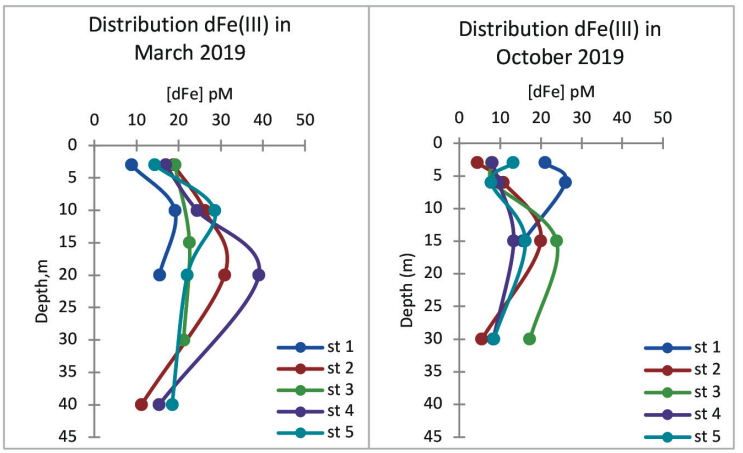

Figure 5: Concentration of dFe(III) in all stations during March 2019 and October 2019 at Redand Island

al. (2006) needed only 30 minutes, 60 minutes, and 90 minutes, respectively, to free the Fe(III) ions from the organic complex in the coastal seawater sample. Thus, this longer irradiation period (Ramjam & Mohamed, 2022) supported the strong organic ligand in our sample.

The potential inputs of these organic ligands were suggested to be produced either by marine microbes such as heterotrophic bacteria and cyanobacteria (Hunter & Boyd, 2007) or by the pore-water from sediments (Jones *et al*., 2011). For our study, we are inclined to suggest that the source of organic ligands in our samples probably comes from the sediment source due to the strong current velocity and rapid mixing processes that has been established during NEM (Godon & Mohamed, 2016), resulting in sediment re-suspension in the water column (Adiana *et al*., 2014). Furthermore, the shallow nature of our study area (≈ 54 m depth) gives the opportunity for sediment inputs without the presence of NEM. However, further study is needed to identify the role of these organic ligands on other dissolved metals' biogeochemistry cycles in our coastal waters.

Conclusions

NEM on the east coast of Peninsular Malaysia was found to affect the physicochemical parameters of seawater, especially salinity, DO, conductivity, and TDS. However, these changes do not affect the distribution of dissolved Fe(III) ions probably due to the presence of strong natural organic Fe(III) binding ligands (FeL). This organic complex maintains the concentration of dissolved Fe(III) ions in the water column throughout the year in the area. However, further study is needed to evaluate the role of these natural organic ligands on other dissolved metals.

Acknowledgements

This project was funded by Universiti Putra Malaysia under Grant Putra (UPM 700-2/1/ GP/2018/9608500). We would like to thank the Ministry of Natural Resources and Environment and Department of Environmental Sciences for the research permit. We are grateful for the assistance from the crew and all the laboratory staff of the Department of Environment, Faculty of Forestry and Environment, UPM during sampling and analysis.

Conflict of Interest Statement

The authors declare that they have no conflict of interest.

References

Abualhaija, M. M., Whitby, H., & van den Berg, C. M. G. (2015). Competition between copper and iron for humic ligands in estuarine waters. *Marine Chemistry*, *172*, 46-56.

Achterberg, E. P., Holland, T. W., & Bowie, A. R. (2001). Determination of iron in seawater. *Analytica Chimica Acta*, *442*(1), 1-14.

Adiana, G., Shazili, N. A. M., & Marinah, M. A. (2014). Effects of northeast monsoon on trace metal distribution in the South China Sea off Peninsular Malaysia. *Environmental Monitoring and Assessment*, *186*(1), 421-431.

Anawat, P., Pradit, S., Sukramongkol, N., & Siriraksophon, S. (2001). Temperature, salinity, dissolved oxygen and water masses of Vietnamese Waters. *Proceedings of the Fourth Technical Seminar on Marine Fishery Resources Survey in the South China Sea, Area IV: Vietnamese Waters*, 346-355.

Barron, J. J., & Ashton, C. (2013). *The effect of temperature on conductivity measurement* [A Reagecon Technical Paper]. County Clare: Ireland.

Boye, M., Aldrich, A. P., Van Den Berg, C. M. G., De Jong, J. T. M., Veldhuis, M., & De Baar, H. J. W. (2003). Horizontal gradient of the chemical speciation of iron in surface waters of the northeast Atlantic Ocean. *Marine Chemistry*, *80*, 129-143.

Boye, M., Aldrich, A., van den Berg, C. M. G., de Jong, J. T. M., Nirmaier, H., Veldhuis, M., Timmermans, K. R., & de Baar, H. J. W. (2006). The chemical speciation of iron in the north-east Atlantic Ocean. *Deep-Sea Research Part I*, *53*, 667-683.

D'Croz, L., & O'Dea, A. (2007). Variability in upwelling along the Pacific shelf of Panama and implications for the distribution of nutrients and chlorophyll. *Estuarine Coastal and Shelf Science*, *73*, 325-340.

Dippner, J. W., & Loick-Wilde, N. (2011). A redefinition of water masses in the Vietnamese upwelling area. *Journal of Marine Systems*, *84*(1-2), 42-47.

Fan Song-Miao. (2008). Photochemical and biochemical controls on reactive oxygen and iron speciation in the pelagic surface ocean. *Marine Chemistry*, *109,* 152-164.

Godon, E., & Mohamed, K. N. (2016). Distribution of Dissolved Fe, Al and Cu at Perhentian Island, Terengganu. In-House Seminar of The Chemical Oceanography Laboratory, *1*(3), 12-18.

Godon, E., Nizam Mohamed, K., Gani, M. A., & Johan, S. (2018). Study of dissolved Copper(II) speciation at coastal water of peninsular Malaysia. *Oriental Journal of Chemistry*, *34*(4), 1858-1877.

Hunter, K. A., & Boyd, P. W. (2007). Iron-binding ligands and their role in the ocean biogeochemistry of iron. *Environmental Chemistry*, *4*, 221-232.

Jack, J. P., Abdsalam, A. T., & Khalifa, N. S. (2009). Assesment of dissolved oxygen in coastal waters of Benghazi, Libya. *Journal of Black Sea/Mediterranian Environment, 15*, 135-156.

Johnson, K. S., Michael Gordon, R., & Coale, K. H. (1997). What controls dissolved iron concentrations in the world ocean? *Marine Chemistry*, *57*, 137-161.

Jones-Lee, A., & Lee, G. F. (2005). Role of iron chemistry in controlling the release of pollutants from resuspended sediments. *Remediation*, *16*(1), 33-41.

Jones, M. E., Beckler, J. S., & Taillefert, M. (2011). The flux of soluble organic-iron(III) complexes from sediments represents a source of stable iron(III) to estuarine waters and to the continental shelf. *Limnology and Oceanography*, *56*(5), 1811-1823.

Klunder, M. B., Laan, P., Middag, R., De Baar, H. J. W., & van Ooijen, J. C. (2011). Dissolved iron in the Southern Ocean (Atlantic sector). *Deep-Sea Research Part II*, *58*, 2678-2694.

Kuma, K., Nishioka, J., & Matsunaga, K. (1996). Controls on iron(III) hydroxide solubility in seawater: The influence of pH and natural organic chelators. *Limnology and Oceanography*, *41*(3), 396-407.

Kumar, P., Singh, A. N., Shrivastava, R., & Mohan, D. (2015). Assessment of seasonal variation in water quality dynamics in River Varuna- A major tributary of River Ganga. *International Journal of Advanced Research*, *3*(3), 1176-1193.

Lin, M., Hu, X., Pan, D., & Han, H. (2018). Determination of iron in seawater: From the laboratory to in situ measurements. *Talanta*, *188*, 135-144.

Lis, H., Shaked, Y., Kranzler, C., Keren, N., & Morel, F. M. M. (2015). Iron bioavailability to phytoplankton: An empirical approach. *The ISME Journal*, *9*, 1003-1013.

Liu, X., & Millero, F. J. (2002). The solubility of iron in seawater. *Marine Chemistry*, *77*, 43-54.

Mandal, H. K. (2014). Effect of temperature on electrical conductivity in industrial effluents. *Recent Research in Science and Technology*, *6*(1), 171-175.

Manikannan, R., Asokan, S., & Ali, A. (2011). Seasonal variations of physico-chemical properties of the Great Vedaranyam Swamp, Point Calimere Wildlife Sanctuary, South-east coast of India. *African Journal*

of Environmental Science and Technology, *5*(9), 673-681.

Martin, J. H., Gordon, R. M., Fitzwater, S. E., Martin, H., Gordon, R. M., & Fitzwater, S. E. (1991). Iron limitation?: The case of iron. *Limnology and Oceanography*, *36*(8), 1793-1802.

Millero, F. J. (1998). Solubility of Fe(III) in seawater. *Earth and Planetary Science Letters*, *154*, 323-329.

Mohamed, K. N., & Amil, R. (2015). Nutrients enrichment experiment on seawater samples at Pulau Perhentian, Terengganu. *Procedia Environmental Sciences*, *30*, 262-267.

Mohamed, K. N., Godon, E., Adnan, N. A., Rahim, Q. A., Liew, C., Abidin, A. I. Z., & Zainuddin, M. F. (2019). Study of dissolved nutrient condition at pulau perhentian, Terengganu. *Pertanika Journal of Science and Technology*, *27*(2), 601-617.

Mohamed, K. N., Ramjam, N. J., & Azahar, N. I. (2021). Dissolved Fe(III) speciation in Tropical Coastal Water: In case of Northeast Monsoon effect. *Journal of Sustainability Science and Management, 16*(8), 256-267.

Muhammad, N., & Mohamed, K. N. (2019). *Determination of cadmium, copper, lead and zinc in particulate phase at Redang Island, Terengganu* [Final Year Project thesis, Universiti Putra Malaysia].

Ngabirano, H., Byamugisha, D., & Ntambi, E. (2016). Effects of seasonal variations in physical parameters on quality of gravity flow water in Kyanamira Sub-County, Kabale District, Uganda. *Journal of Water Resource and Protection*, *8*(13), 1297-1309.

Pan, X. F., Yan, B. X., & Muneoki, Y. (2011). Effects of land use and changes in cover on the transformation and transportation of iron: A case study of the Sanjiang Plain, Northeast China. *Science China Earth Sciences*, *54*(5), 686-693.

Prabu, V. A., Rajkumar, M., & Perumal, P. (2008). Seasonal variations in physico-chemical characteristics of Pichavaram mangroves, southeast coast of India. *Journal of Environmental Biology*, *29*(6), 945-950.

Ramjam, N. J., & Mohamed, K. N. (2022). Optimisation of Dissolved Fe(III) determination in coastal water by using electrochemistry approach and 2, 3-Dihydroxynaphthalene as the binding ligand. *International Journal of Electrochemical Science*, *16*(21091), 1-18.

Roseli, N. H., Akhir, M. F., Husain, M. L., Tangang, F., & Ali, A. (2015). Water mass characteristics and stratification at the Shallow Sunda Shelf of Southern South China Sea. *Open Journal of Marine Science*, *5*(4), 455-467.

Saravanakumar, A., Rajkumar, M., Serebiah, S. J., & Thivakaran, G. A. (2008). Seasonal variations in physico-chemical characteristics of water, sediment and soil texture in arid zone mangroves of Kachchh-Gujarat. *Journal of Environmental Biology*, *29*(5), 725-732.

Shoukat, A., Hussain, M. S., & Shoukat, A. (2020, February). *Effect of Temperature on Total Dissolved Solid in Water* [Conference Paper]. Water Quality Study: Water Treatment and Recycling, Mehran University Sindh, Pakistan.

Syed Jamaludin, S. S., Wan Zin, W. Z., Mohd Deni, S., & Jemain, A. A. (2010). Trends in Peninsular Malaysia rainfall data during the southwest monsoon and northeast monsoon seasons: 1975-2004. *Sains Malaysiana*, *39*(4), 533-542.

Vijayakumar, S., Rajesh, K., Mendon, M., & Hariharan, V. (2000). Seasonal distribution and behaviour of nutrients with reference to tidal rhythm in the Mulki Estuary, South-West Coast of India. *Journal of Marine Biological Association of India*, *42*(1&2), 21-31.

Wilson, P. C. (2010). Water quality notes: Dissolved oxygen. *IFAS Extension*, 1-8.

Zainol, Z., & Akhir, M. F. (2016). Coastal upwelling at Terengganu and Pahang coastal waters: Interaction of hydrography, current circulation and phytoplankton biomass. *Jurnal Teknologi*, *78*(8), 11-27.

Zhu, Y., Hu, X., Pan, D., Han, H., Lin, M., Lu, Y., Wang, C., & Zhu, R. (2018). Speciation determination of iron and its spatial and seasonal distribution in coastal river. *Scientific Reports*, *8*(2576), 1-9.